

## N O T I C E

THIS DOCUMENT HAS BEEN REPRODUCED FROM  
MICROFICHE. ALTHOUGH IT IS RECOGNIZED THAT  
CERTAIN PORTIONS ARE ILLEGIBLE, IT IS BEING RELEASED  
IN THE INTEREST OF MAKING AVAILABLE AS MUCH  
INFORMATION AS POSSIBLE

RICE UNIVERSITY

"EVAPORATIVE COOLING ON A GROOVED SURFACE"

by

Dwight Yoder

A THESIS SUBMITTED  
IN PARTIAL FULFILLMENT OF THE  
REQUIREMENTS FOR THE DEGREE

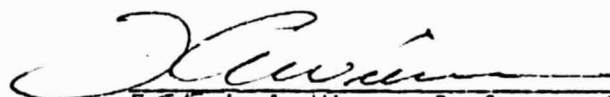
Master of Science

(NASA-CR-160410) EVAPORATIVE COOLING ON A  
GROOVED SURFACE M.S. Thesis (Rice Univ.)  
42 p HC A03/MP A01 CSCL 20D


N80-13401

Unclas  
G3/34 42718

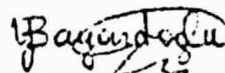
APPROVED THESIS COMMITTEE:



Frédéric A. Wierum, Professor of Mechanical Engineering and Thesis Director



Alan J. Chapman, Professor of Mechanical Engineering and Dean of Engineering



Yildiz Bayazitoglu, Assistant Professor of Mechanical Engineering

HOUSTON, TEXAS

MAY 1979

# "EVAPORATIVE COOLING ON A GROOVED SURFACE"

by

Dwight Yoder

## Abstract

Spray evaporative cooling defines a mode of heat transfer where the drops evaporate on contact with the heated surface. Since no water accumulates on the surface, the term "dry wall" is used to describe the surface condition. If while operating in the dry-wall mode the surface temperature is lowered, there will be a transition to a point where water will begin to accumulate on the surface. When water begins to accumulate the surface is said to be "flooded".

Behavior at this transition point was investigated experimentally to determine the temperatures and corresponding heat flux at which this transition occurred. Several pressure ranges were considered including one below the triple point of water. Additionally, the results using a grooved surface were compared to those using a smooth surface. It was determined that a grooved surface has no effect on the heat transfer.

ACKNOWLEDGMENTS

This project was funded through NASA Grant NAS9-65274. The contract monitor was Luis Trevino of the Crew Systems Division of the National Aeronautics and Space Administration, Johnson Space Center.

Special thanks goes to Professor Frederic A. Wierum, Principal Investigator and Thesis Director for the time and effort he spent on the project.

The author is grateful to his wife, Carolyn Yoder, for her help in data reduction, preparing the figures and for the general support she offered.

Thanks is also due the department secretaries, Marla Wells and Nancy Wolff for typing done for this project.

TABLE OF CONTENTS

	<u>Page</u>
ABSTRACT	i
ACKNOWLEDGMENT	ii
TABLE OF CONTENTS	iii
NOMENCLATURE	iv
I. INTRODUCTION	1
II. ANALYSIS OF SPRAY COOLING	3
III. EXPERIMENTAL APPARATUS	5
A. Heat Flux and Temperature Measurement	5
B. Spray System	6
C. Vacuum System	7
IV. EXPERIMENTAL PROCEDURE	9
V. DATA ANALYSIS	12
VI. EXPERIMENTAL RESULTS AND DISCUSSION	14
REFERENCES	21
FIGURES	23

NOMENCLATURE

C	Specific heat
K	Thermal Conductivity of aluminum sample
$\dot{m}$	Mass flow rate/unit area
q	Heat flux
$T_b$	Base temperature
$T_s$	Saturation temperature
$T_w$	Wall or surface temperature
$\lambda$	Latent heat
$\lambda^*$	$C(T_s - T_f) + \lambda$

## INTRODUCTION

The purpose of this work is to study the heat transfer characteristics of a spray mist (water) impinging on a horizontal surface. Interest in this work is on the case where water is evaporated as it contacts the surface; no water accumulates on the surface. This condition is defined as "dry-wall". In particular, interest lies in determining the wall temperature (and corresponding heat flux) at which the dry-wall mode ceases to exist and water begins to accumulate on the surface. "Flooding" is used to define the condition where water begins to accumulate on the surface.

This behavior is to be investigated for several pressure ranges varying from just below the triple point to atmospheric conditions. Previous work on this project resulted in data for a smooth surface (aluminum) [1]. Current work involves comparing results from a grooved (or finned) surface to the previous results. The data base will also be extended.

Motivation for the current study is the heat rejection system selected by the National Aeronautics and Space Administration for use in the Space Shuttle (Fig. 1). Heat rejection in this system involves spray mist cooling near the flooding point. Operation is slightly below the triple point.

Considerable previous work has been done in the area of heat transfer to drops and in systems that use a spray in some manner. A limited number of references will be cited. Studies concerning heat transfer characteristics of sessile drops, impinging (single) drops,

mists and thin films have been made [2-9]. Much work has been done on heat transfer in the Leidenfrost mode [10-13]. Droplet behavior on impingement has been studied [14].

However, none of the above work studies the heat transfer characteristics at the transition between dry-wall and flooding. And thus, previous work is not directly applicable to the present study. Very little work has been done at low pressure.

Industrial applications of spray mist cooling would arise when cooling must be accomplished using a minimum amount of coolant or in processes which require cooling at a very low pressure.



### ANALYSIS OF SPRAY COOLING

Before beginning discussion of the experimental results it is necessary to consider the possible behavior of the mist as it contacts the surface. In particular, a brief discussion of the dry-wall mode, flooded mode, and Leidenfrost mode.

Heat transfer in the dry-wall state is quite easy to predict. Since the droplets are evaporated upon contact with the surface (no accumulation), the heat transfer is just the energy needed to raise the drop to the saturation temperature ( $T_s$ ) plus the energy needed to vaporize the drop. In general, subcooling at low pressure will be zero or, at least, negligible. Therefore, the heat transfer at low pressure ( $< 20$  mm Hg) is given by

$$q = \dot{m} \lambda$$

Subcooling effects at atmospheric pressure will be more significant ( $\approx 10-15\%$ ). The heat transfer at atmospheric pressure is given by

$$q = \dot{m} \lambda^*$$

Obviously there will be a point at which the surface cannot support dry-wall conditions. Water will arrive at the surface faster than it can be evaporated and will begin to accumulate on the surface. Heat transfer with water on the surface is much harder to predict. Modes of heat transfer in this flooded state will be one or more types

of boiling depending on the surface temperature ( $T_w$ ) and  $T_s$ . The purpose of the present work is not to study the behavior in the flooded mode extensively, but, rather, to investigate experimentally at what wall temperature this flooding occurs and to determine the corresponding heat transfer.

Determining this flooding point is especially important for pressure ranges at or below the triple point of water. Excess water at a pressure below the triple point creates a potential freezing problem. This freezing initiates at points on the surface that are cooler than the rest of the surface, and tends to propagate from these points until ice covers the remaining surface.

Behavior at the Leidenfrost state, as mentioned earlier, has been studied extensively. The only interest here is to determine the approximate Leidenfrost point. This point is made obvious by the drop behavior on the surface. The drops may bounce off of the surface or move across the surface at a rapid rate. Heat transfer in this mode is much less than in the other two modes.

## EXPERIMENTAL APPARATUS

As was mentioned in the general analysis it is necessary to measure the heat flux, surface temperature, and saturation temperature (or pressure). Before presenting details, consider the general experimental set-up (Fig. 2). The various components will now be described.

### Heat Flux and Temperature Measurement

Shown in Figure 3 is the schematic of the heat flux sample. Dimensions of grooves are given in Figure 10a. Nine copper-constantan thermocouples (TC) were placed at 1/4" intervals along the specimen (6061-T6 aluminum) centerline. The TC were placed in 1/16" holes drilled to the center of the specimen. The first TC was placed 1/4" from the surface. Two additional TC placed 1/4" from the surface but at a radial distance from the center were used to check that a one-dimensional temperature profile did indeed exist. All TC were formed using Leeds and Northrup "Quicktip" TC connectors. The holes in the sample were filled with Wood's metal (M.P. 80°C) to insure good thermal contact between the TC and the specimen.

Thermocouple voltages were measured several ways. Either a chart recorder (Heath model SR-206) or Omega Digital Thermometer Type 2809 were used. Both of these were constantly checked and calibrated with a millivolt potentiometer (I. & N #8662). Temperature measurements were accurate to within 0.3°C.

Energy was supplied via a 400 W commercial cartridge heat (Chromalox CIR-3020), inserted in the base of the specimen. A commercial temperature controller (Omega Model 49T) was used to keep the base temperature ( $T_b$ ) (i.e., the temperature of TC #9) at a constant temperature. The output of TC #9 was used as feedback to the controller. The controller worked on a completely off or completely on basis, resulting in either 0 V or 120 V applied to the heater. This proved to make a constant base temperature very difficult to maintain. To correct the problem the output of the controller was connected to a Variac. This allowed the voltage delivered to the heater to be varied. Adjustment of the Variac to a point where the controller had to be "on" almost all of the time allowed an essentially constant  $T_b$  at equilibrium.

#### Spray System

The spray was supplied at approximately 20°C through a 0.4 mm D, 45° included angle, full cone nozzle. Distilled water was supplied from a 9-gallon low-pressure storage vessel. Air at 25 psig provided the pressure over the water. The flow rate was controlled with a needle valve. Observations of the spray cone indicated that at low pressure the cone was essentially hollow with drop size appearing to be uniform. At atmospheric pressure the cone was full, but drops were not of uniform size. Indirect measurement of flow rate was provided by a ball-in tube rotameter.

No attempt was made to measure the droplet size at low pressure. With the system under the bell jar, space limitations did not allow such measurements to be made. Gayle [15] has suggested that the droplet

size in a vacuum is controlled by the pressure. That is, the droplets adjust in size to reach an equilibrium between internal, surface tension, and external forces. Previous work on this project yielded a droplet distribution at atmospheric pressure [1]. (See Figure 4)

#### Vacuum System

The bell jar was 18 in. diameter, 30 in. high with a stainless steel base plate. Wire and fluid passages were provided through the plate [17]. Vapor generated was frozen in a nitrogen-cooled cold trap. This provided some protection for the vacuum pump from condensable vapors. In addition it provided a vapor-pump effect which was especially useful at pressures below the triple point.

Different orifice sizes used at the exit duct of the bell jar allowed pressure (in the jar) to be maintained over several distinct ranges. Following are the average pressures for the orifices used.

<u>Orifice #</u>	<u>Dia (cm)</u>	<u>Average Pressure (mm Hg)</u>
1	.318	20.18
2	.953	7.11
(triple pt.)		4.587
3	1.588	4.51

Pressure was measured in several ways. It was determined that the environment under the jar at all operating conditions was at saturated conditions. This was done by placing two thermometers such that the mist would contact them. The pressure was then measured using either a diaphragm pressure gage (MKS Instruments, "Baratron" 0-1000  $\mu$ m Hg), a McLeod gage (Stokes 0-5000  $\mu$ m Hg), or a single tube manometer (Merian 0-250 mm Hg). The average temperature always corresponded

to the saturation temperature for the measured pressure. Thereafter, the thermometer readings were used to obtain the pressure (checks were constantly made with the pressure measuring devices). Below the triple point ice formed on the thermometers. Therefore, the pressure below the TP was measured with the McLeod gage.

EXPERIMENTAL PROCEDURE

Nozzle positioning to provide the appropriate spray mass flux to the sample surface proved to be the most difficult task. When a different heat flux was desired it was necessary to change the height and/or tilt of the nozzle. The nozzle had to be positioned to provide the mass flux necessary for the desired heat flux range. In addition (and this was the difficult part), the nozzle had to be positioned such that the spray was uniform over the surface. It would be undesirable to have a significant portion of the surface flooding while the other was basically dry. Adjusting the flow rate served as a fine adjustment. It required considerable effort and experience to adjust the nozzle correctly.

With the nozzle positioned, the next step was to adjust the temperature controller (and therefore heat flux) to obtain the desired surface conditions. If for a given spray, the surface was too dry the base temperature would be slowly lowered until flooding just began. Likewise, if the surface was initially too wet,  $T_b$  would be raised slowly until the desired conditions were achieved. When the surface was at the desired condition the Variac would be adjusted to make  $T_b$  as stable as possible.

Output voltages from TC #1 (surface) and TC #9 (base) were continuously monitored via the chart recorder. When both of these voltages (temperatures) were constant, equilibrium conditions had been reached. With the surface at the desired conditions and the system in the equilibrium a temperature profile could be taken. The chart recorder also recorded the temperature profile. After the profile was taken conditions were rechecked to make sure the system was still in equilibrium.

Before the above procedure could be implemented to yield a "good" data point, it was necessary to determine what the conditions of flooding were. Since the interest was in determining the "flooding" point, it was necessary to define conditions where "dry-wall" becomes "flooded". Flooding for the smooth surface was defined as the point where small pools just began forming on the surface [1]. However, for the grooved surface flooding was more difficult to define. The difficulty arose in determining how much, if any, water standing in the grooves constitutes "flooding". In addition, during the experiments the surface was under the bell jar so close observation was difficult. That is, it was not easy to tell exactly how much water was in the grooves. Flooding was finally defined to be a point where some water could be standing in the grooves, but never enough to allow spanning of a groove.

Figures 5,6,7 can be used to better describe flooding conditions. Water did not stand along the entire length of the groove. The depth of the water averaged over the length of groove probably never exceeded  $1/3$  of the groove height. No condition near spanning (Fig. 7) was allowed over a significant portion of the surface. It must be emphasized that these appeared to be general or average conditions at the flooding point. There were, possibly, considerable variations. To compensate for this variation in flooding conditions a considerable number of data points were taken.

The criterion for determining the flooding point was not entirely arbitrary. It was desired to define the flooding point to allow as large a heat flux as possible without running the risk of obtaining



excess fluid on the surface.

Some effort was spent in trying to observe the surface through a telescope. While not as successful as hoped, certain observations were made. When the drops hit the surface they appeared to evaporate right there. That is, no movement of the drops, such as sliding down the groove, was noticed.

The above procedure was followed for each data point obtained. Prior to each day's run the surface was cleaned with a soft brush.

DATA ANALYSIS

The result of the foregoing experimental procedure was a profile of TC voltage along the length of the sample. From this it was necessary to determine the heat flux and temperature at the surface.

Rather than laboriously using the TC tables and interpolating, the table was fitted to a cubic equation:

$$T = 31.9583 + 46.64386X - 1.28737X^2 + .052205X^3$$

X = TC voltage in mV

This equation agreed with the table to 0.1°F for  $30 \leq T \leq 245^\circ\text{F}$  which was sufficient for the precision of the other data. Thus the temperature gradient along the sample could be obtained.

As was expected the temperature gradient was a straight line. A linear regression was performed to obtain the value of the gradient. The intercept given by the linear regression was the wall temperature. A typical value of the correlation coefficient was .9995. Figure 8 shows a typical profile.

Previous work yielded an expression for the thermal conductivity of 6061-T6 aluminum as [1,16]

$$K(T) = 92.82 + 8.184(10^{-2})T - 4.144(10^{-4})T^2 \quad \frac{\text{B}}{\text{hr}\cdot\text{ft}\cdot^\circ\text{F}}$$

With the values of the temperature gradient and the thermal conductivity, the heat flux was determined by

$$q = K \frac{dt}{dx}$$

The entire analysis was done on a programmable calculator (TI-58).

EXPERIMENTAL RESULTS AND DISCUSSION

Figure 9 shows the data for orifice #2 ( $\bar{P} = 7.11$  mm Hg). This pressure range was chosen to compare the ridged and the smooth surface. This choice was made because more data for the smooth surface was available in this range. Scatter in the data was taken to be a result of not being able to define the flooding point in a perfectly consistent manner. As can be seen, the data for the ridged surface follows the line for the smooth surface.

This result warrants some discussion since, in general, an increase in surface area is associated with an increase in heat transfer. However, there are a couple of important differences between common heat exchanger conditions and the conditions of the present work. Usually there is an excess of fluid on the heat exchanger surface. Contrasting this is the current work which seeks to avoid excess fluid (flooding). Also, heat transfer is usually in the form of sensible heat.

There are two explanations for the observed behavior. The first is purely geometrical. Consider a control surface over a groove and the corresponding smooth surface area (Fig. 10b). When the smooth surface is at impending flooding (but still at dry-wall) there is a fixed number of droplets passing through the control surface. A simple addition of grooves will not increase the heat transfer because

$$q = \dot{m} \lambda$$

at dry-wall conditions. To increase  $q$  the mass flux would have to be

increased. But this would require a fine adjustment of the spray. In fact, it would be difficult, if not impossible, to adjust the spray to take advantage of all of the extra area.

Additionally, the temperature distribution in the fin must be considered. Temperatures along the fin will be less than the base temperature of the fin (which is  $T_w$ ). Thus, the droplets will impinge on a surface which has a temperature lower than  $T_w$ . Now, when heat is transferred by sensible heat, it is only necessary that the surface in contact with the fluid be at a higher temperature than the fluid. However, in the present case,  $T_w$  must be sufficiently greater than  $T_s$  so that the drop is vaporized before the next drop arrives. Since the drops are hitting a surface with a temperature lower than  $T_w$ , flooding will begin earlier (i.e., less spray per unit area) than if the entire fin were at  $T_w$ .

A boiling curve was taken for orifice #2. Excess water was sprayed on the surface. Attempts were made to establish a film over the surface. However, a film could not be maintained. At low  $\Delta T(T_w - T_s)$ , large pools formed which were in constant violent action. At higher  $\Delta T$ , pools were smaller and moved very fast over the surface. Figure 11 shows the boiling curve compared to the impending flooding data for orifice #2.

While the purpose of this work was not to study boiling at low pressure, a few comments about some observations might be useful for future work. During the course of taking this boiling curve the drain for the excess water plugged up causing water to build up over the surface. However, when this excess water covered the surface (a little less than 1 cm deep), the heat flux changed very little, if at all,

from what it had been when the conditions were just that of excess water (but no standing film). The water that covered the surface boiled violently.

It should be noted that this accidental flooding occurred occasionally during the course of this work (that is in gathering the regular data). In some cases the heat flux changed very little as described above. Occasionally, though, this flooding changed the heat flux drastically sometimes raising and sometimes lowering it. No general correlations were made between the effect of this flooding and the other parameters.

Figure 12 shows the data for orifice #3 ( $\bar{P} = 4.51$  mm Hg). This data does not define a straight line as well as the orifice #2 data did. For the same value of  $\Delta T$  significantly different heat flux values were obtained. This scatter is not due to the difficulty in determining the exact conditions of the flooding point. The scatter in the data is much too severe to be accounted for in this manner. An alternate explanation is needed.

The explanation involves the "definition" of the saturation temperature of water below the triple point (the liquid is actually in a metastable state). Saturation temperature of the water below the triple point was taken as  $0^{\circ}\text{C}$ . While it may be argued that the saturation temperature may not be at a constant  $0^{\circ}\text{C}$ , it is difficult to justify the use of another value (or values).

With the saturation temperature a constant, a plot using  $\Delta T$  is essentially a plot using  $T_w$ . However, there can be many values of the heat flux for a given  $T_w$ . It only requires a change in the

mass flow rate. To understand this, consider the method used to evaluate  $q$ . A temperature profile was obtained along the sample. This gradient along with the thermal conductivity yielded  $q$ . There could be many temperature gradients with the same intercept (i.e.,  $T_w$ ). (See Fig. 13). Thus, with  $T_s$  a constant, a plot of  $q$  vs.  $\Delta T$  could be expected to have scatter.

As was mentioned earlier, excess water can lead to freezing at pressures below the triple point. Freezing on the heated surface was not expected and did not occur. However, at values of  $\Delta T$  approximately equal to  $15^\circ\text{C}$  and lower, freezing would begin at the interface of the surface and the teflon insulation. The ice formation would then move inward over the surface (Fig. 14). Spray that was supposed to hit the surface would, instead, hit this ice creating yet more ice. The danger in having excess water on the surface (even a large drop) is that drops were observed to move off of the surface on to the teflon. Even with a large surface this could still prove to be a problem because the drop could move to a part of the surface that was cooler than the main surface. Freezing could then begin there and spread over the other parts of the surface.

It is important to note that once freezing begins it cannot be stopped by increasing the control temperature at the base of the sample (i.e., by increasing the heat flux). The only way to halt the freezing is to increase the pressure in the bell jar (i.e., by raising the saturation pressure to a value above the triple point). With the present set-up this was accomplished most effectively by admitting small amounts of air into the system. Melting would begin almost immediately. This proved to be an effective means of controlling

the freezing problem.

Prior to taking data for orifice #1 ( $\bar{P} = 20.2$  mm Hg), it was expected that the increased pressure would increase the saturation temperature but that the behavior would be similar to orifice #2. The data (Fig. 15) show that this is not the case, however. In fact there are similarities in the behavior of orifice #3 and orifice #1.

To understand the behavior at the different pressure ranges it is necessary to understand the relationship between the heat flux and the pressure in the bell jar. Additionally, the relationship between saturation temperature and saturation pressure is needed. When the heat flux is increased, the amount of vapor generated is increased. This increased vapor causes an increase in pressure under the bell jar. This increased pressure in turn causes an increase in  $T_s$ .

Saturation temperature vs. saturation pressure is plotted in Figure 16. Indicated on this plot is the average pressure for each orifice. As mentioned earlier  $T_s$  was taken as  $0^\circ\text{C}$  for pressures at or below the triple point. Therefore, there was (by definition) no variation of  $T_s$  with  $P_s$  ( $\frac{dT_s}{dP_s} = 0$ ). However,  $\frac{dT_s}{dP_s}$  for the pressure range given by orifice #2 is almost twice what it is for the range provided by orifice #1.

Thus, a given  $\Delta P$  produces a larger  $\Delta T_s$  for orifice #2 than for orifice #1. Now consider the effect of an increase of  $\Delta T_s$  on the system. If  $T_s$  increases while  $T_w$  remains constant (or if  $T_w$  changes at a rate slower than the rate of change of  $T_s$ ),  $\Delta T$  becomes smaller. Thus the temperature gradient must be adjusted so that when the system again reaches equilibrium the surface is at the desired



conditions. This is a complicated process and cannot at present be described quantitatively. The above discussion allows a qualitative understanding of the behavior.

Comparing the results of the three orifices shows that the lower the value of  $\frac{dT_s}{dP_s}$  the higher is the attainable heat flux for a given  $\Delta T$ . That is for a given  $\Delta T$  orifice #3 provides the highest attainable heat flux followed by orifice #1 and finally by orifice #2. This is just the result of the behavior discussed above. When  $\frac{dT_s}{dP_s}$  is large it is necessary to allow a larger  $\Delta T$  to reach equilibrium for a given heat flux.

Data taken at atmospheric pressure are compared to data for the smooth surface in Figure 17. As can be seen, once again, the grooves make no difference at the impending flooding point. However, the grooves were expected to improve the heat transfer in boiling. They, in fact, increased the heat transfer to such an extent that it was not possible to take a boiling curve with the present apparatus. (It was possible to take a boiling curve with the smooth surface.)

No attempt was made to study the Leidenfrost point extensively. However, several times during the course of the work a Leidenfrost point was observed. This information is shown in the following table. It must be remembered these are very limited observations and should be treated as such. Consider also that the literature on the subject shows that the Leidenfrost point has wide variations depending on how the drops hit the surface, material of surface, etc.

<u>Orifice #</u>	<u>P (mm Hg)</u>	<u>Leidenfrost <math>\Delta T</math> (C)</u>
1	20.20	58
2	7.11	55
3	4.51	69

Future work should study other parameters such as droplet size and velocity. The effect of pulsing the spray and the effect of changing inlet water temperature are currently under study. In addition, more knowledge is needed concerning the low pressure behaviour of nozzles.

REFERENCES

1. Grissom, Bill, "A Fundamental Study of Spray-Evaporative Cooling," M.S. Thesis, Rice University, May 1979.
2. McGinnis, F.K. and J.P. Holman, "Individual Droplet Heat-Transfer Rates for Splattering on Hot Surfaces," Int. J. Heat Mass Transfer, Vol. 12, 95-108 (1969).
3. Michiyoshi, Itaru and Kunchide, Makino, "Heat Transfer Characteristics of Evaporation of a Liquid Droplet on Heated Surfaces," Int. J. Heat Mass Transfer, Vol. 21, 605-613 (1978).
4. Toda, S., "A study of mist cooling - thermal behaviors of liquid film formed from mist drops on a heated surface at high temperatures and high heat fluxes," Tohoku Univ. Technology Reports, Vol. 36, No. 2, (1971).
5. Toda, S. and H. Uchida, "Study of liquid film cooling with evaporation and boiling," Heat Transfer - Japanese Research, Vol. 2, No. 3, (1973).
6. Bonancina, C., G. Comini and S. Del Guidice, "Evaporation of atomized liquids on hot surface," Letters in Heat and Mass Transfer, Vol. 2, pp. 401-406 (1975).
7. Finlay, I.C., "An analysis of heat transfer during flow of an air-water mist across a heated cylinder," The Canadian Journal of Chemical Engineering, Vol. 49, (June 1971).
8. Yang, W.-J., "Mechanics of droplet evaporation on heated surfaces," Letters in Heat and Mass Transfer, Vol. 5, pp. 151-166 (1978).
9. Kopchikov, I.A., G.I. Voronin, et al., "Liquid boiling in a thin film," Int. J. Heat Mass Transfer, Vol. 12, pp. 791-796 (1969).
10. Bell, K. J., "The Leidenfrost phenomenon: a survey," Chem. Eng. Prog. Symposium Ser., Vol. 63, p. 73 (1967).
11. Gottfried, B.S., C.J. Lee and K.J. Bell, "The Leidenfrost Phenomenon: film boiling of liquid droplets on a flat plate," Int. J. Heat Mass Transfer, Vol. 9, pp. 1167-1187 (1966).
12. Rao, P.S.V.K. and P.K. Sarma, "Effect of sub-cooling on film boiling heat transfer: droplet evaporation on a hot plate," Journal of Chemical Engineering of Japan, Vol. 7, No 5, (1974).

13. Hoogendoorn, C. J. and R. den Hord, "Leidenfrost temperature and heat transfer coefficients for water sprays impinging on a hot surface," Proc. 5th Int. Heat Transfer Conf., Tokyo (1974).
14. Savic, P. and G.T. Bault, "The fluid flow associated with the impact of liquid drops with solid surfaces", National Research Council of Canada, rep. nr. MT-26, (May 1955).
15. Gayle, John, et.al. "Freezing of Liquids on Sudden Exposure to Vacuum," Journal of Spacecraft, Vol. 1, No. 3, (May-June) 1964.
16. "Aluminum-properties," Physical Metallurgy, P.D., Kent R. Van Horn, ed., Alcoa, P. 7, (1967).
17. Shero, J.P. "Porous Plate Sublimator Analysis," Phd. Thesis, Rice University, November, 1969.

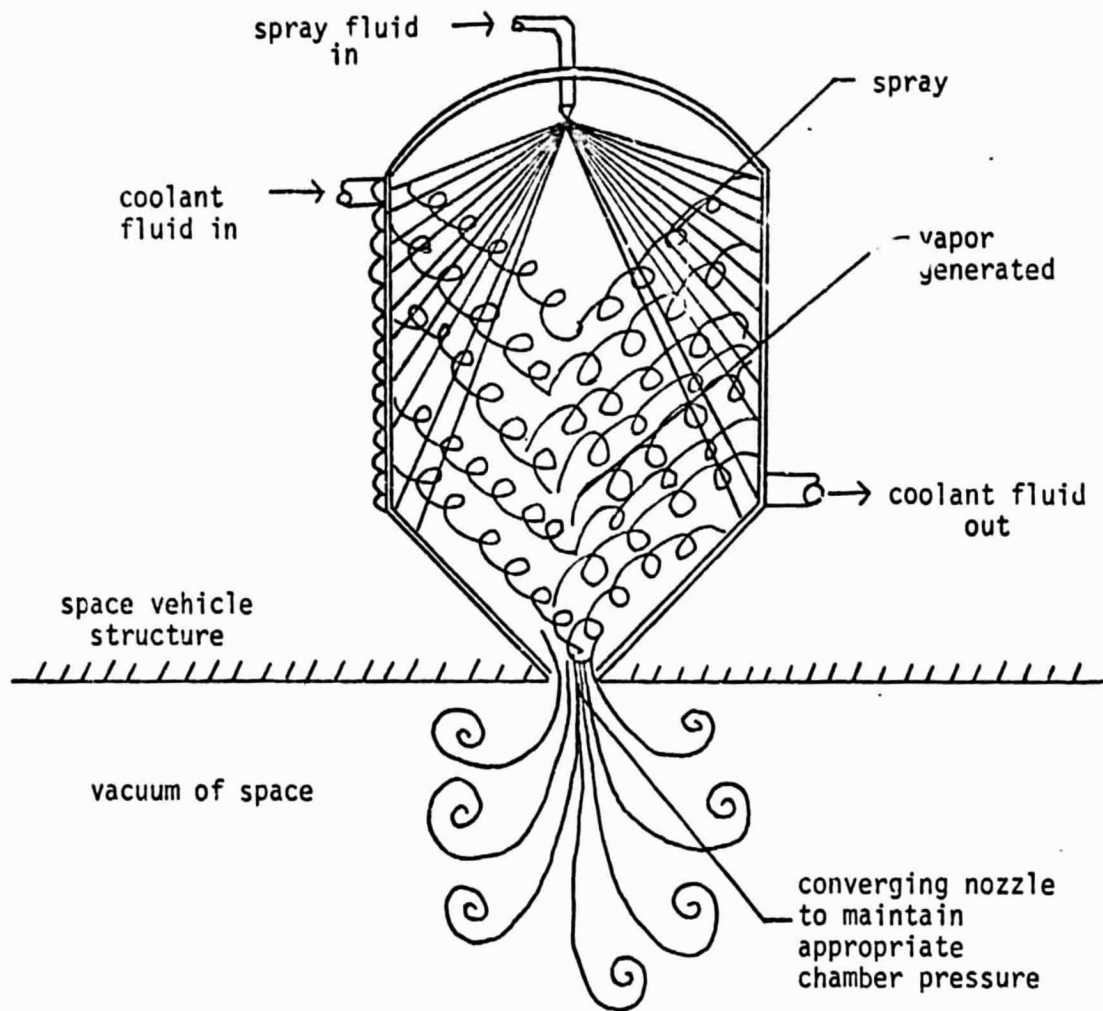


Figure 1. Operation of NASA's "Flash Evaporator System"

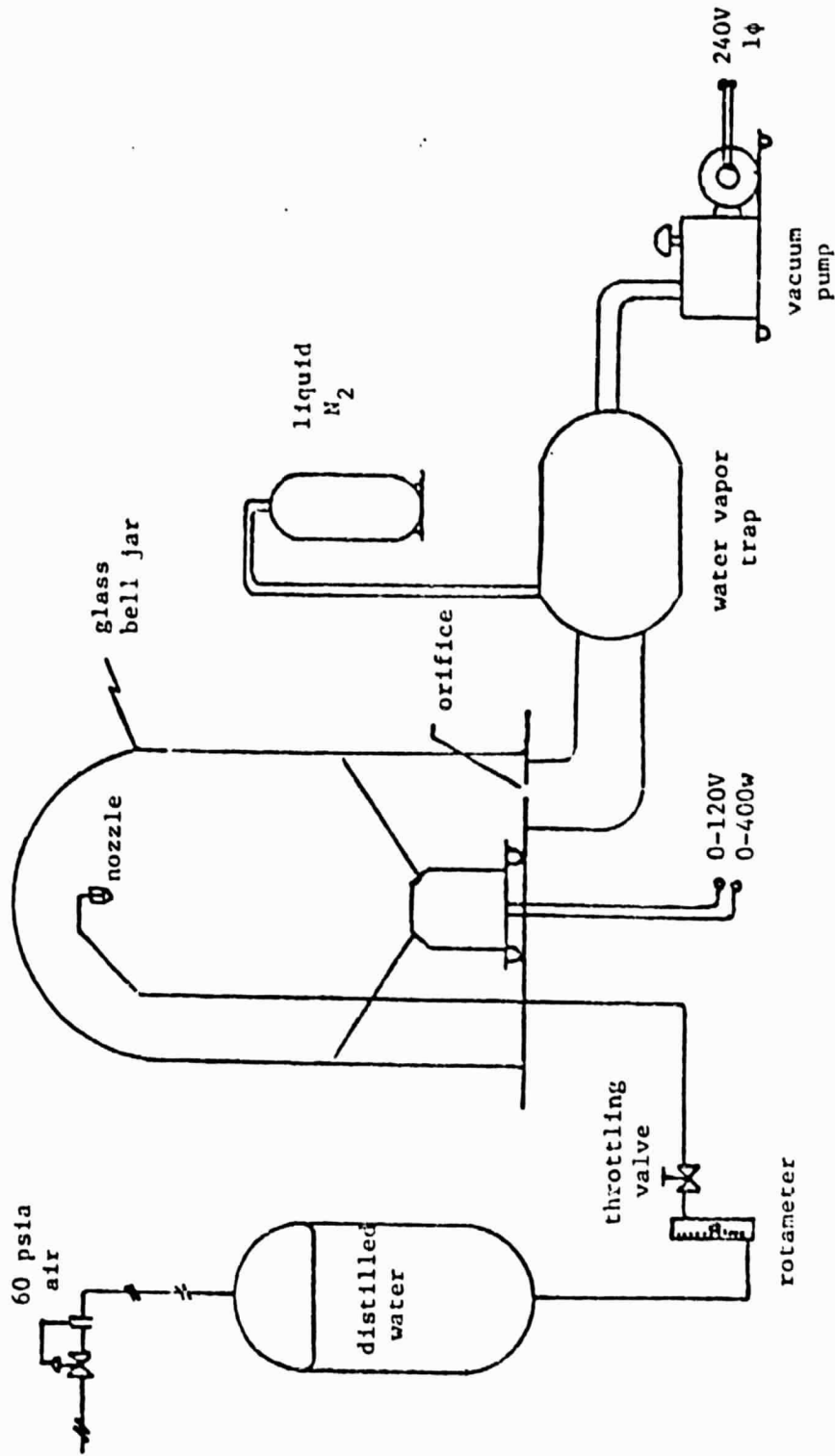


FIGURE 2. Schematic diagram of vacuum system and liquid spray supply. [1]

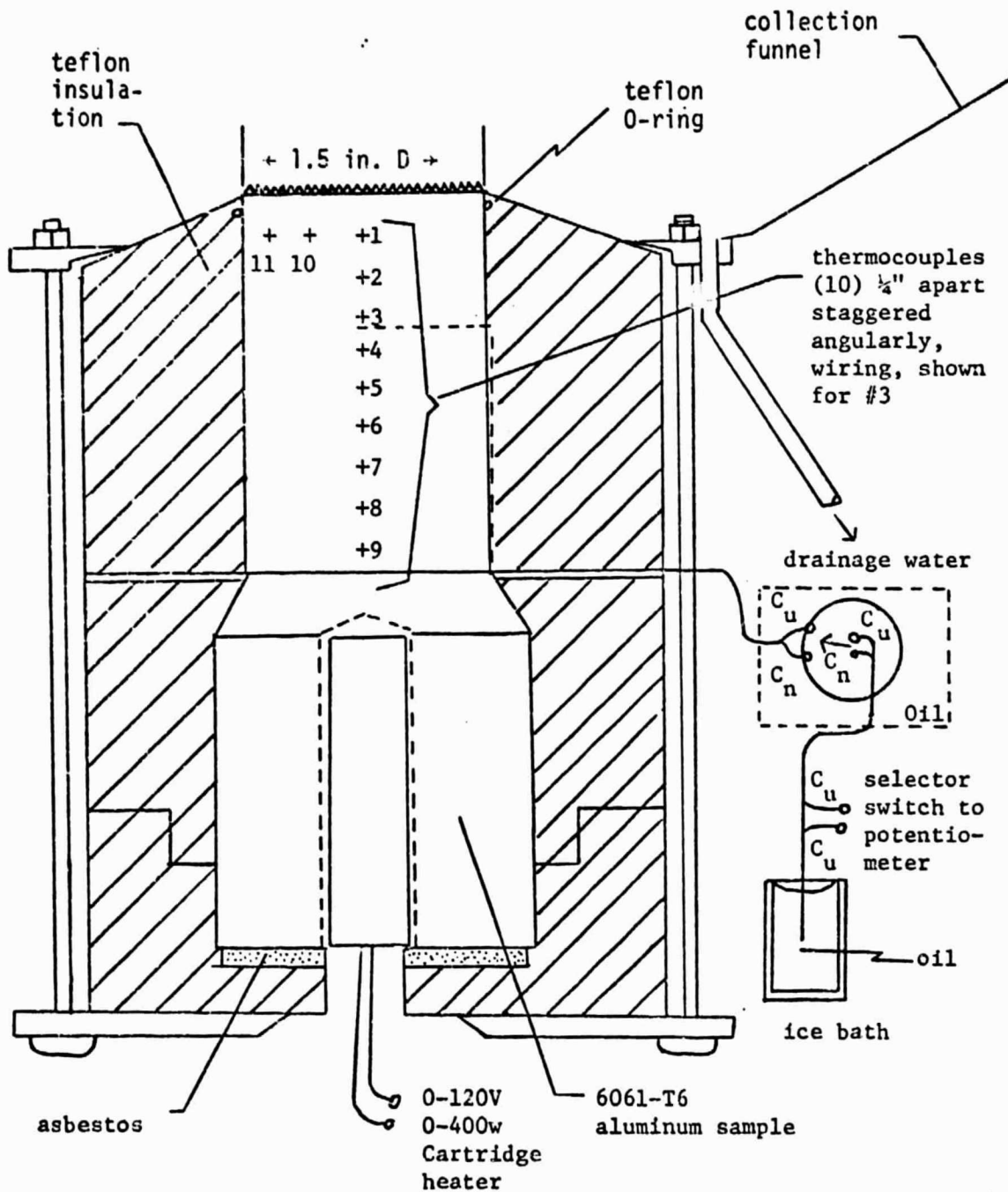


FIGURE 3. Schematic diagram of the heat flux sample. [1]

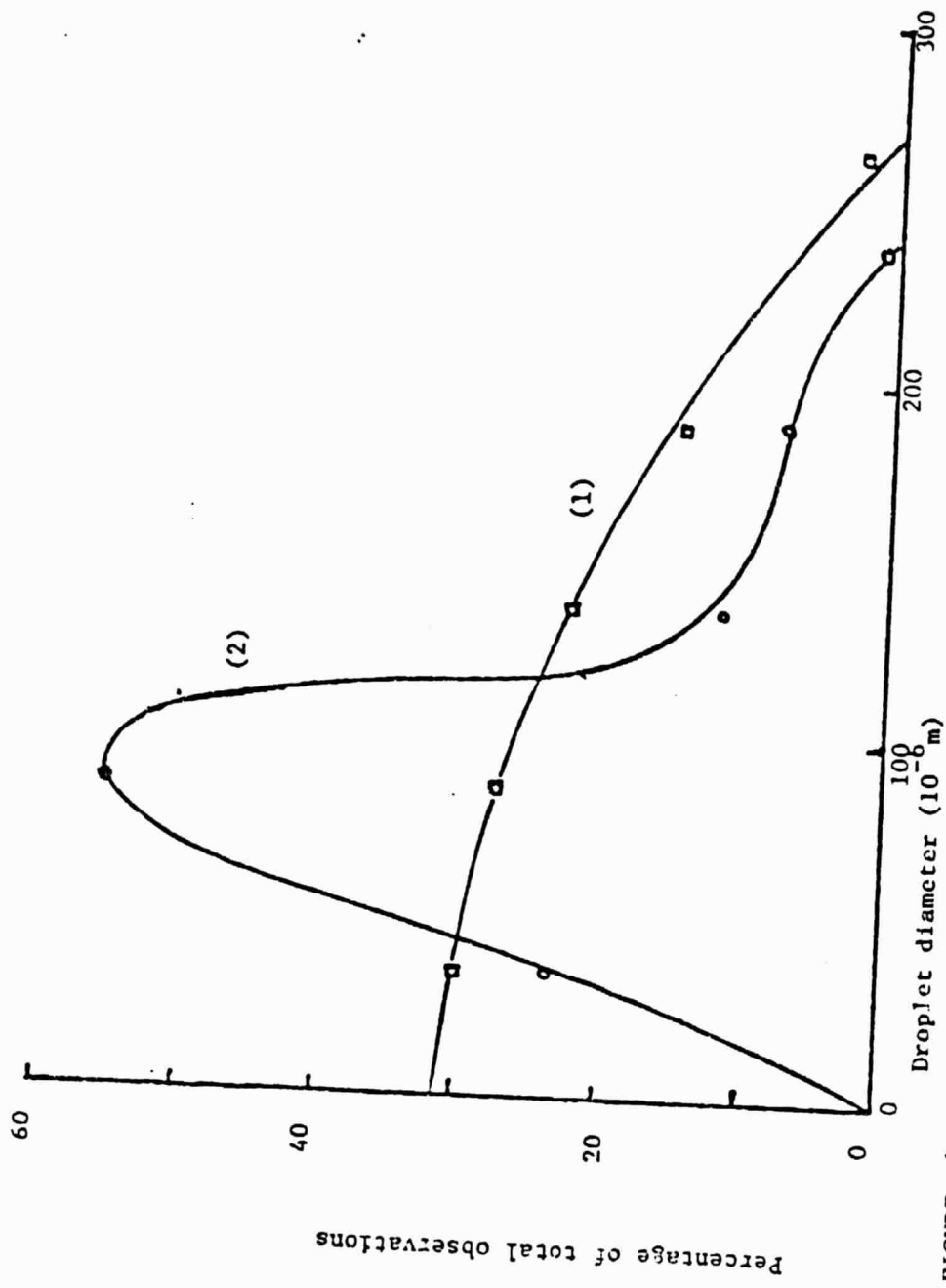


FIGURE 4. Droplet size distribution: (1) center of spray, (2) fringe of spray. [1]

Percentage of total observations



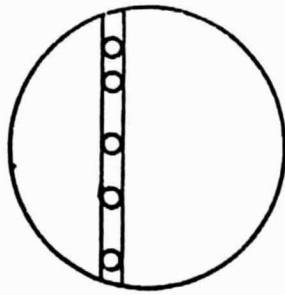


FIGURE 5.



FIGURE 6.

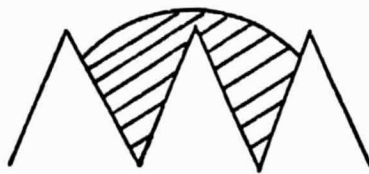


FIGURE 7.

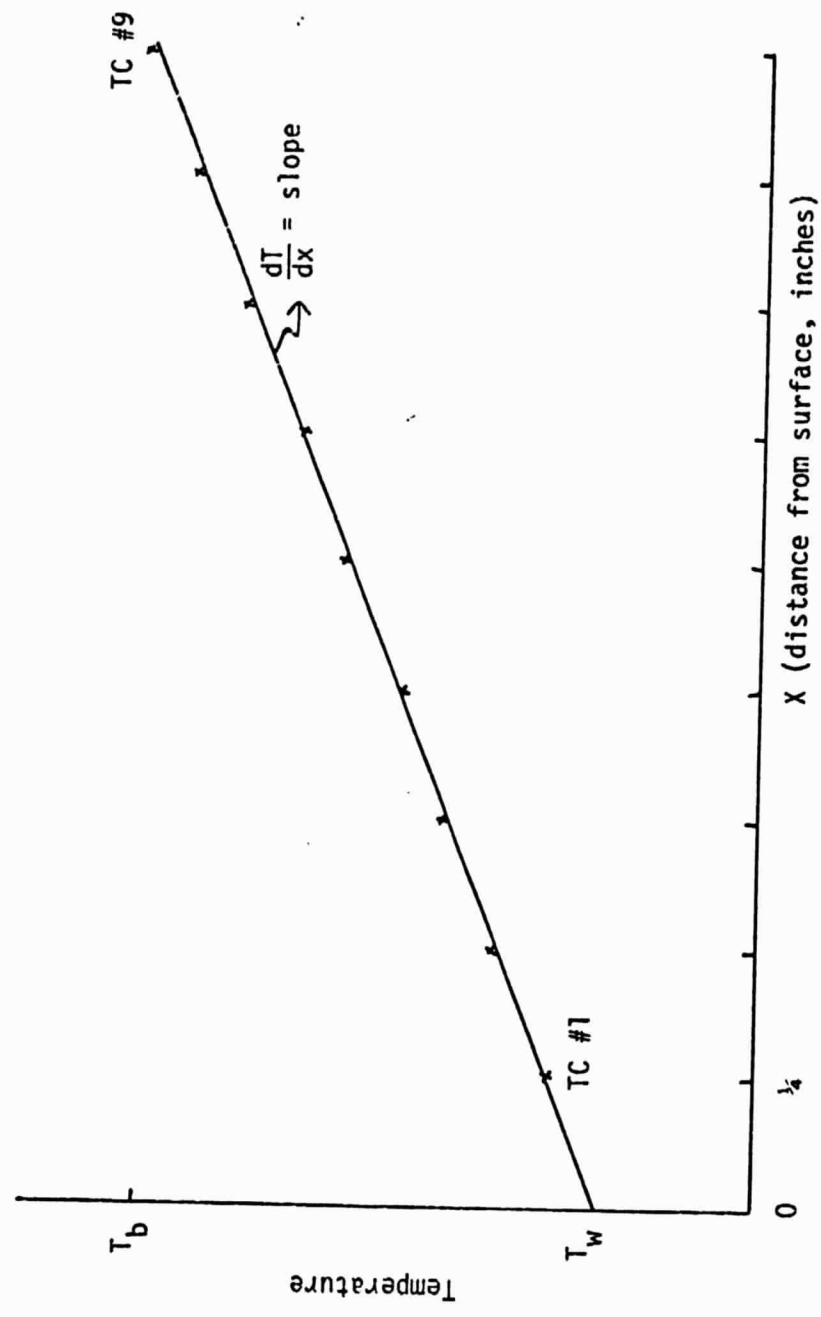


FIGURE 8. Typical temperature profile.

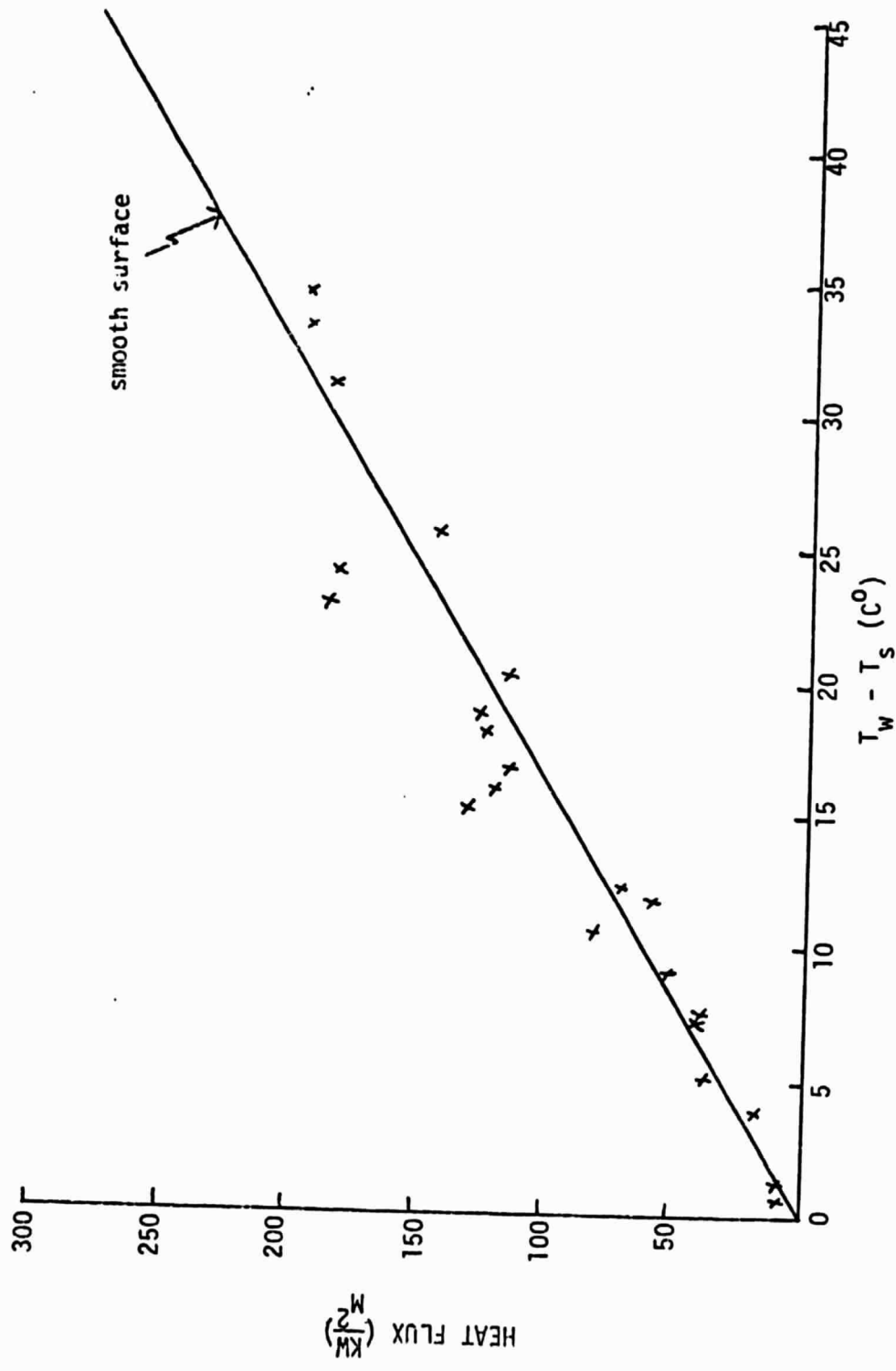


FIGURE 9. Flooding data for orifice #2 ( $\bar{P} = 7.11$  mm Hg)

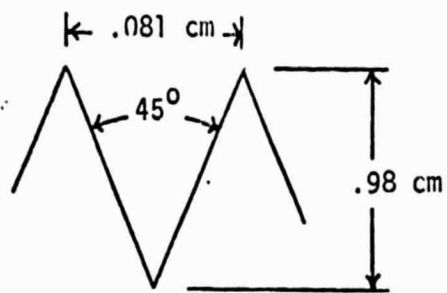


FIGURE 10a. Dimensions of ridges.

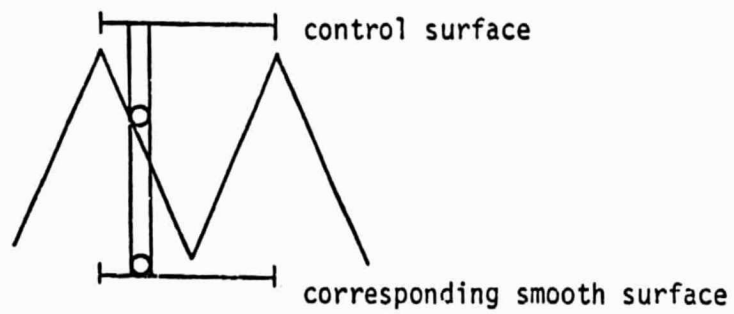


FIGURE 10b.

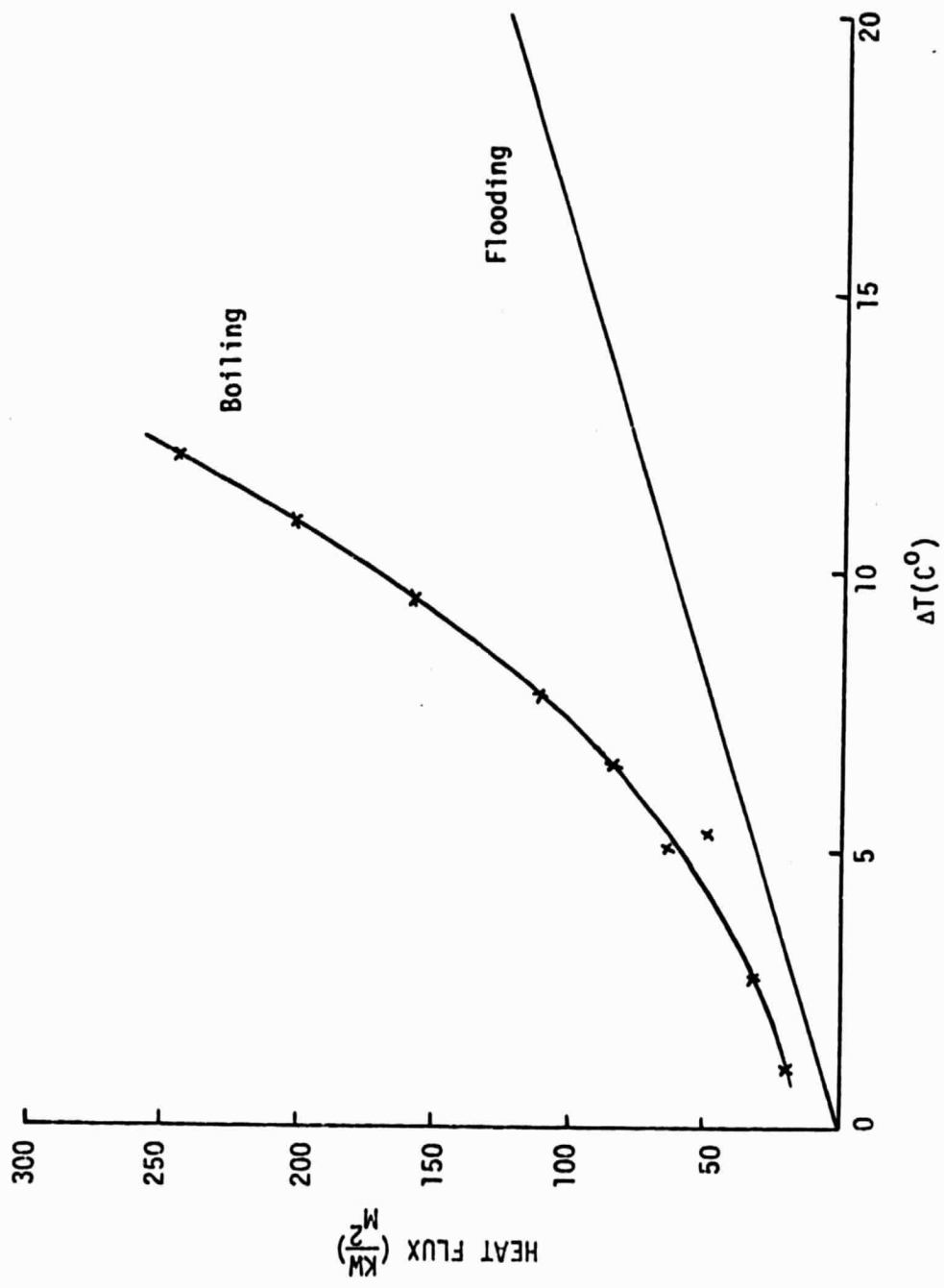


FIGURE 11. Orifice #2 ( $\bar{P} = 7.11$  mm Hg). Boiling compared to Flooding.

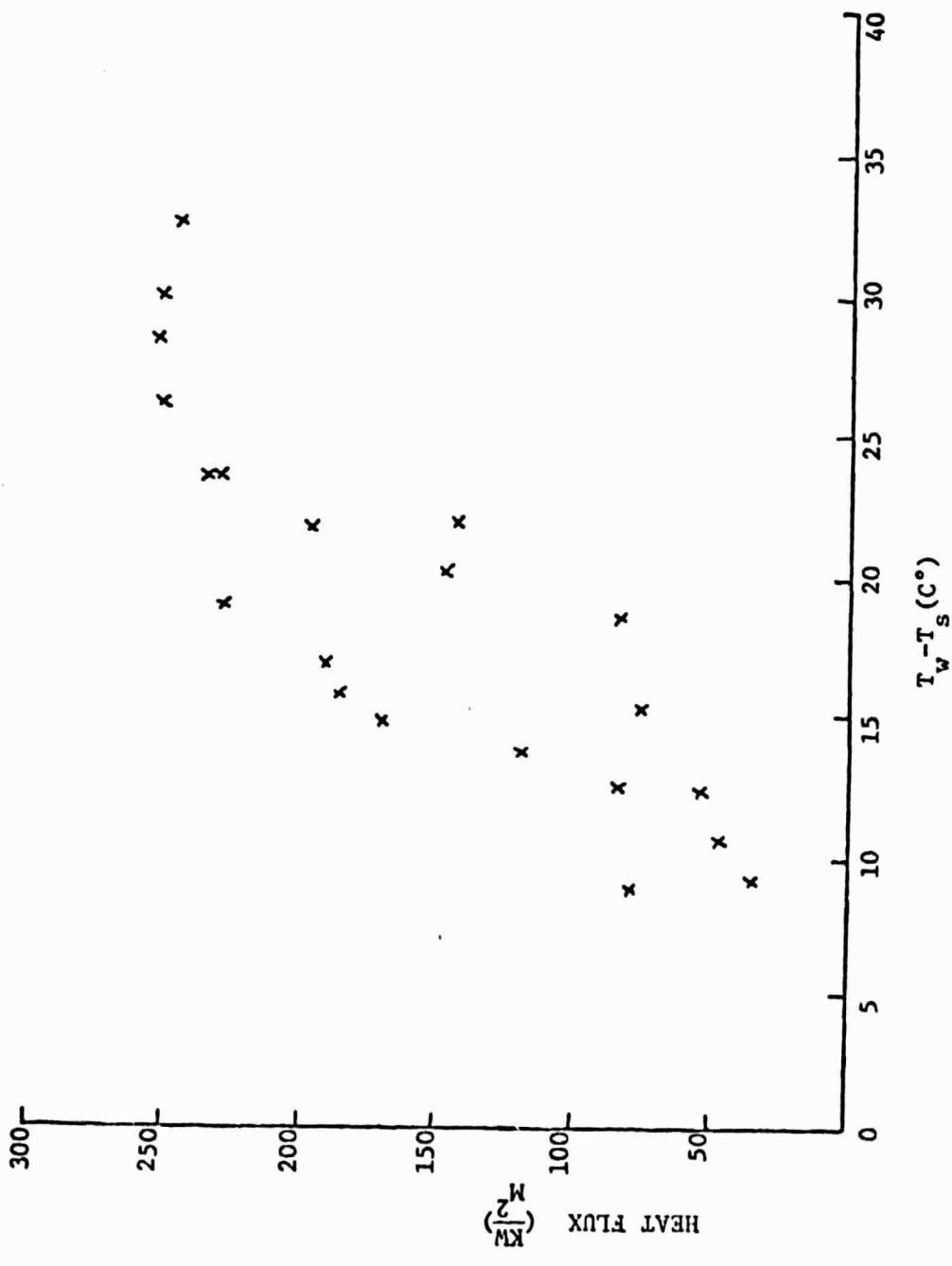


FIGURE 12 . Flooding data for orifice #3 ( $\bar{P} = 4.51$  mm Hg).

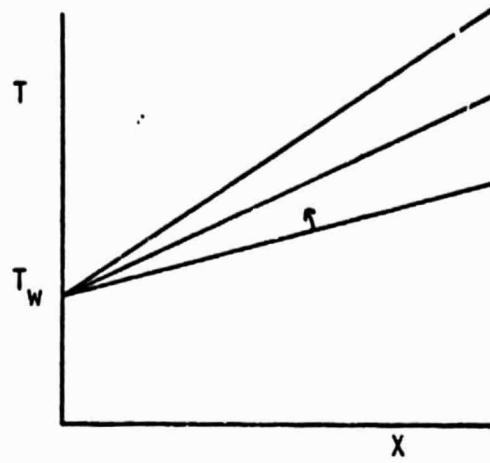


FIGURE 13. Profile behavior below the triple point.

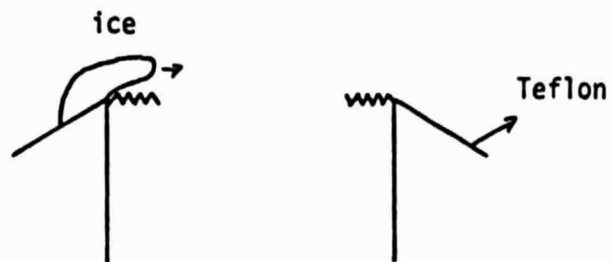


FIGURE 14. Ice formation.

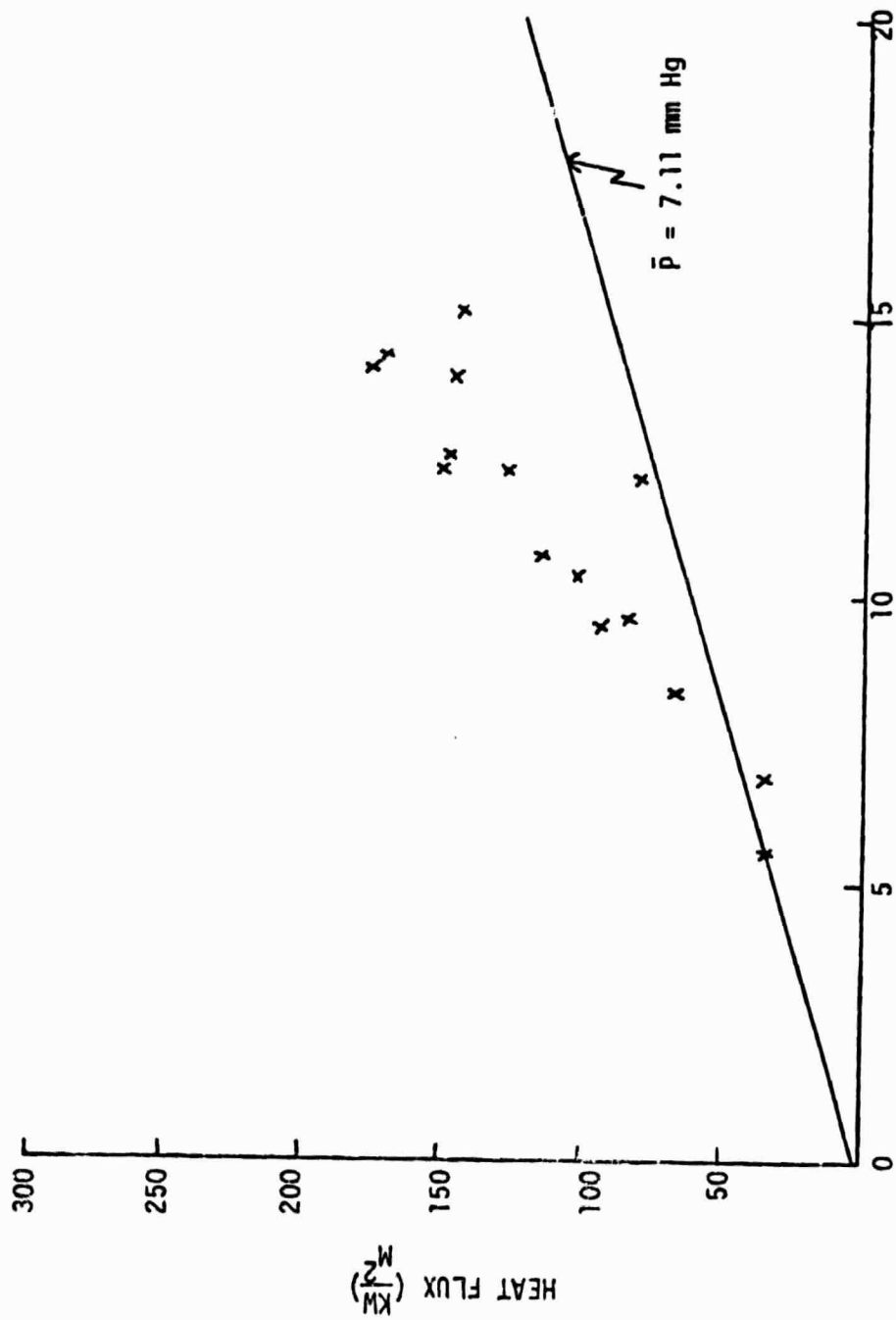
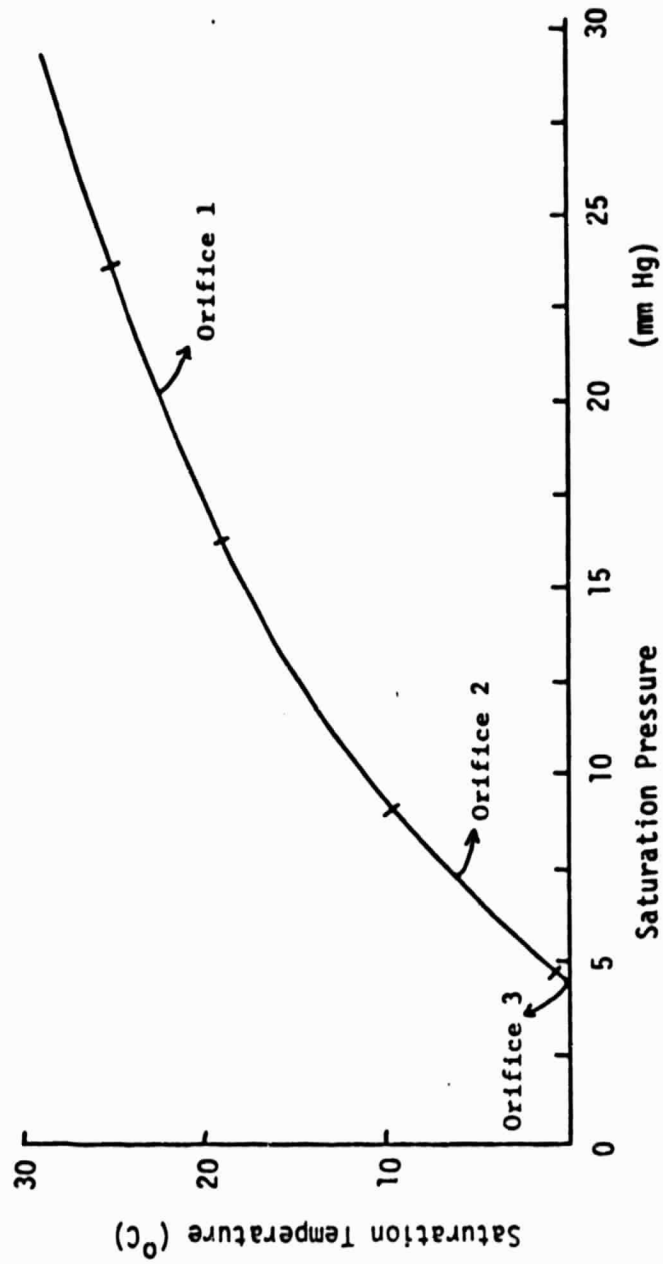


FIGURE 15. Flooding data for orifice #1 ( $P = 20.18 \text{ mm Hg}$ ).



FIGURE 16.  $T_s$  vs.  $P_s$  for water.

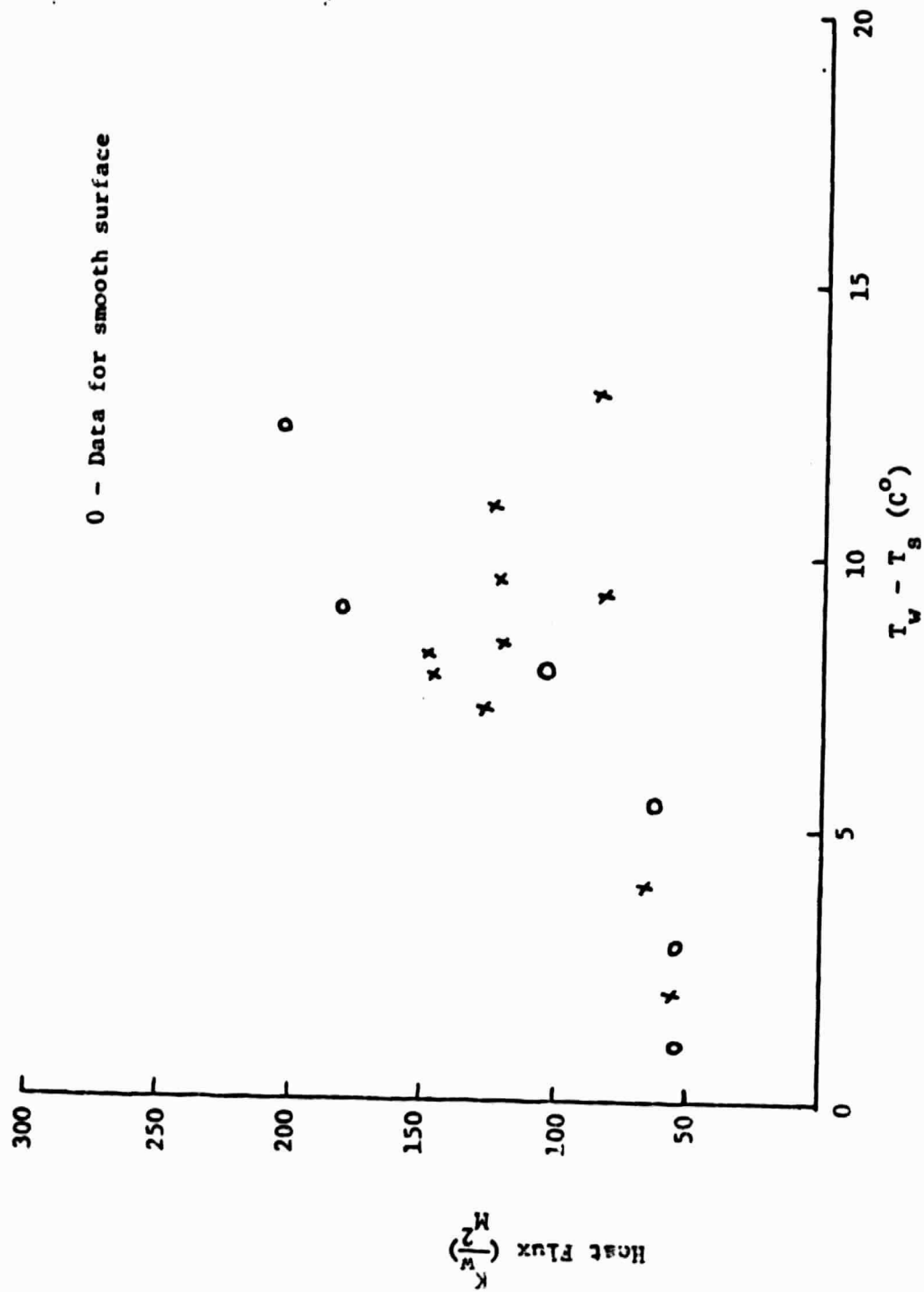


FIGURE 17. Flooding data at atmospheric pressure.